Discrete Sampling of Extreme Events Modifies Their Statistics

Lior Zarfaty,[1,*] Eli Barkai,[1] and David A. Kessler[2]
[1]Department of Physics, Institute of Nanotechnology and Advanced Materials, Bar-Ilan University, Ramat-Gan 52900, Israel
[2]Department of Physics, Bar-Ilan University, Ramat-Gan 52900, Israel

(Received 27 September 2021; revised 25 April 2022; accepted 27 July 2022; published 25 August 2022)

Extreme value (EV) statistics of correlated systems are widely investigated in many fields, spanning the spectrum from weather forecasting to earthquake prediction. Does the unavoidable discrete sampling of a continuous correlated stochastic process change its EV distribution? We explore this question for correlated random variables modeled via Langevin dynamics for a particle in a potential field. For potentials growing at infinity faster than linearly and for long measurement times, we find that the EV distribution of the discretely sampled process diverges from that of the full continuous dataset and converges to that of independent and identically distributed random variables drawn from the process's equilibrium measure. However, for processes with sublinear potentials, the long-time limit is the EV statistics of the continuously sampled data. We treat processes whose equilibrium measures belong to the three EV attractors: Gumbel, Fréchet, and Weibull. Our Letter shows that the EV statistics can be extremely sensitive to the sampling rate of the data.

DOI: 10.1103/PhysRevLett.129.094101

Introduction.—Extreme value (EV) statistics is a venerable branch of probability theory, which has drawn much interest over the years [1–5]. It finds diverse application not only in physics [6–40], but in many other fields of science as well [41–58]. Predicting when the next EV event will occur and of what magnitude it will be is of practical importance, as the extremes are typically the scenarios we are looking forward to, or alternatively, must watch out for [26,27,43,44,54]. Hence, a thorough understanding of EV statistics is crucial. The EV distribution arising from independent and identically distributed (IID) random variables (RV) has various limiting laws when the sample size approaches infinity [59–63], in a similar way to central limit theorems for sums of IID RVs [64]. More precisely, the nature of the tail of the underlying distribution of the IID RVs determines the limiting form of the scaled EV's distribution to be either of Gumbel, Fréchet, or Weibull form. However, it is clear that for many natural processes, correlations are vital and omnipresent [34], hence the assumption that one is dealing with IID RVs is, in most cases, simply wrong [7,12,19,20,26,29,37,39].

Typically, one measures an extreme of a time series that represents some quantity, be it for example a temperature [55], the value of a currency [57], or the position of an active biological entity [58]. In principle, the series is continuous, and EV models of such continuously sampled (CS) stochastic paths have attracted considerable attention. However, in reality, for any experimental study the amount of data collected and the sampling rate of the measurement devices are both always finite. Thus, the approach that is relevant to real-world applications is to first discretely sample (DS) the path, and then find the maximum of the sampled sequence of data. Is there a major difference between these two sampling methods?

In this Letter, we answer this question in the context of correlated trajectories of a Brownian particle in a force field, modeled by Langevin dynamics. We start with one of the most well-investigated stochastic processes, the Ornstein-Uhlenbeck (OU) model (see also Refs. [30,65]). It describes the motion of an overdamped particle in a harmonic field or, equivalently, the velocity of a damped Brownian particle. Naively, if the time between sampling events is shorter than the relaxation time, then the former should not be expected to play a major role, and we expect to get the CS EV statistics. But, as we show here, for any finite sampling interval this is wrong.

Our remarkable finding is a qualitative nonsmooth transition from DS to CS in the statistics of extremes, which we present first using the OU model. It exists for any positive sampling interval when the overall measurement time is increased, and is not related to a physical change of the system. It strongly affects the mean and variance of the EV distribution, and thus also the typical fluctuations and large deviations of the EVs [38]. Nevertheless, for the OU process both DS and CS give rise to a Gumbel distribution for the EV, in the limit of infinitely long observation time; see below.

We then extend our results to a wide class of Langevin processes that lie in the Gumbel domain, unveiling a second transition governed by the large-displacement behavior of the force field controlling the dynamics. Finally, within this Langevin approach, we briefly present in the Appendix extensions to processes whose equilibrium distributions (ED) belong to the other two EV limits, Fréchet and Weibull.

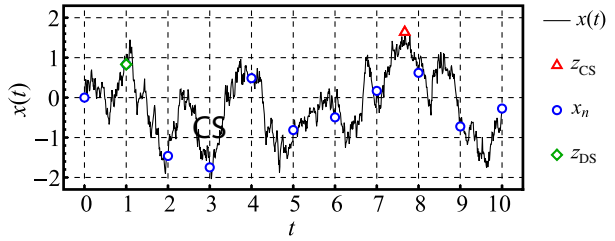

FIG. 1. A piece of an OU trajectory. The path of a Brownian particle in a confining harmonic force field, modeled via the OU process (solid curve). This path's maximum is $z_{\rm CS}$ (red triangle), while discretely sampling every $\Delta = 1$ unit of time yields the sequence x_n (blue circles), with a maximum of $z_{\rm DS}$ (green diamond).

The OU model.—We start by considering the Langevin equation for the OU model,

$$\frac{d}{dt}x(t) = -\frac{1}{\tau}x(t) + \sqrt{2D}\eta(t), \tag{1}$$

where τ, D, and $\eta(t)$ are the relaxation time, the diffusion coefficient, and standard Gaussian white noise, respectively. The noise obeys $\langle \eta(t)\eta(t')\rangle = \delta(t-t')$ and has zero mean, where $\delta(\cdot)$ is Dirac's delta function. The particle, at position $x(t)$, is subject to a force which is derived from a quadratic potential. We rescale all quantities in the equation such that t and $x(t)$ are measured in units of τ and $\sqrt{D\tau}$, respectively. We specialize to this OU path $x(t)$ in the time interval $[0, T]$, and sample it stroboscopically every Δ units of time; see Fig. 1. The outcome of this DS measurement is the random sequence $x_n \equiv x(n\Delta)$, where $0 \le n \le N$ and $N\Delta = T$ is the total measurement time. We focus on the maximum of this set, denoted $z_{\rm DS}$, and compare its properties to those of the previously studied case of the maximum of $x(t)$ in the interval $[0, T]$, $z_{\rm CS} \equiv \max_{0\le t\le T}[x(t)]$ [34,66]. To compute this latter quantity, one has to measure the whole continuous trajectory, and hence we call it the CS model. Clearly, $z_{\rm DS} \le z_{\rm CS}$.

The binding force ensures that an ensemble of particles will reach a steady state, the Boltzmann-Gibbs measure, given by $\phi(x) \equiv \exp(-x^2/2)/\sqrt{2\pi}$. In the limit of large Δ and T but fixed N, the sampling is of uncorrelated RVs all drawn from the ED. Thus, if $z_{\rm DS} < z$ then all the N sampled variables are also smaller than z, and since they are IID RVs drawn from the ED we find that $\lim_{\Delta\to\infty}{\rm Prob}(z_{\rm DS} < z) = [\Phi(z)]^N$, with $\Phi(z) \equiv \int_{-\infty}^{z} dx\, \phi(x) = 1 - {\rm erfc}(z/\sqrt{2})/2$ and ${\rm erfc}(\cdot)$ is the complementary error function. In this limit, the nature of the EV statistics is only due to the equilibrium properties of the system, and any dynamical information, including correlation effects, is wiped out. When N is large, the typical EVs are also large [38]; hence we assume $z \gg 1$, where $\Phi(z) \simeq 1 - z^{-1}\phi(z)$, and get

$$\lim_{\Delta\to\infty}{\rm Prob}(z_{\rm DS} < z) \sim \exp\left[-Nz^{-1}\phi(z)\right]. \tag{2}$$

To treat the DS EV case, we consider the positions x_n at the moments of sampling using a discrete stochastic map. By integrating the Langevin equation, Eq. (1), one finds the OU update formula, $x_{n+1} = \mu x_n + \sqrt{1-\mu^2}\eta_n$, where the η_ns are standard Gaussian IID deviates and $\mu \equiv \exp(-\Delta)$ [67]. In the large-N limit, we find

$${\rm Prob}(z_{\rm DS} < z) \sim A(z)\exp\left\{-N\ln\left[\frac{1}{\Lambda_*(z)}\right]\right\}. \tag{3}$$

The amplitude $A(z)$ approaches unity for large z and the main focus here is the largest eigenvalue, $\Lambda_*(z)$. The latter obeys the following integral equation, obtained from the stochastic map [68],

$$\Lambda_*(z)P_*(x;z) = \int_{-\infty}^{z}\frac{dx'\,P_*(x';z)}{\sqrt{2\pi(1-\mu^2)}}\exp\left[-\frac{(x-\mu x')^2}{2(1-\mu^2)}\right], \tag{4}$$

where $P_*(x;z)$ is the corresponding eigenfunction. Evaluating the joint limit of $\Delta \to 0$ and $N \to \infty$ with T fixed and large [68], we obtain the Fokker-Planck description of the problem, $\lim_{\Delta\to 0}{\rm Prob}(z_{\rm DS} < z) \sim \exp[-T\lambda_*(z)]$, i.e., the CS limit, with $\lambda_*(z) \equiv \lim_{\Delta\to 0}[1-\Lambda_*(z)]/\Delta$. In Ref. [34], it was shown that $\lambda_*(z)$ is the smallest magnitude solution of $D_{\lambda_*(z)}(-z) = 0$, $D_\cdot(\cdot)$ being the parabolic cylinder function, a result which we recover. For large z, one has $\lambda_*(z) \sim z\phi(z)$ [70], and the CS limit becomes [34,66]

$$\lim_{\Delta\to 0}{\rm Prob}(z_{\rm DS} < z) \sim \exp\left[-Tz\phi(z)\right]. \tag{5}$$

The Gaussian decay of the exponents in Eqs. (2) and (5) means that both the IID and CS limits belong to the Gumbel universality class. However, the large-z asymptotic behavior of these two exponents differs by a diverging factor of z^2, making the corresponding EV distributions vastly different. Surprisingly, for any finite Δ, the large-N limit of the DS process's EV distribution, Eq. (3), which is dominated by the large-z asymptotics of the eigenvalue $\Lambda_*(z)$, converges to the EV measure given by the ED IID limit, both for the OU process along with a wide class of similar processes, as we show below. Hence, the limit of $\Delta \to 0$ is singular in the context of EV theory [71].

To begin analyzing the DS EV problem, we use a small-μ (or equivalently, large-Δ) perturbation theory, expanding $\Lambda_*(z) = \sum_{n=0}^{\infty}\lambda_n(z)\mu^n$, and similarly for $P_*(x;z)$. Using Eq. (4), we get that $\Lambda_*(z) \simeq \Phi(z) + \mu[\phi(z)]^2/\Phi(z)$ to first order in μ. For large-z this implies that

$$\Lambda_*(z) \simeq 1 - z^{-1}\phi(z) + \mu[\phi(z)]^2. \tag{6}$$

The second term is expected as it is the result obtained for IID RVs that originate from the ED. A key observation is that for large z, the third term is by far smaller than the

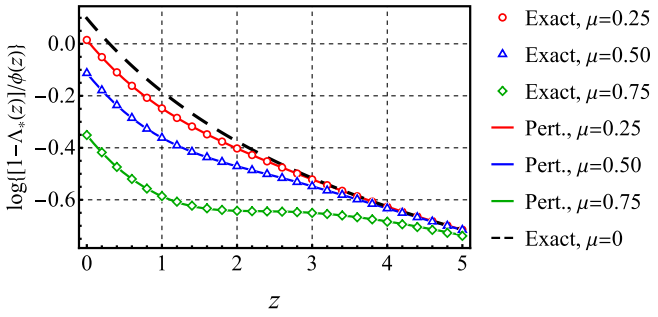

FIG. 2. The large-z convergence of $\Lambda_*(z)$. The scaled eigenvalue $[1-\Lambda_*(z)]/\phi(z)$ for $\mu \equiv \exp(-\Delta) = 0.25$ (red circles), $\mu = 0.5$ (blue triangles), and $\mu = 0.75$ (green diamonds), obtained from numerical evaluations of the eigenvalue equation, Eq. (4), as well as from a tenth-order perturbative expansion in μ (solid curves). Also shown is the exact result for the IID case, $\mu = 0$, for which $\Lambda_*(z) = \Phi(z)$ (dashed black line). Notice that all three finite-μ curves merge for large z with the IID line.

second one, even if μ is not too small, since $\phi(z) \ll 1$. The first-order correction with μ is thus exponentially small in z with respect to the leading term. We continue the small-μ expansion to order 10 [72] and find, similarly, that all the terms up to μ^{10} are negligible in the large-z limit. This behavior is also found in numerical calculations of the eigenvalue $\Lambda_*(z)$ [68], as exhibited in Fig. 2, showing that for large values of z all the numerical data converge to a unique curve which is Δ independent, namely the IID curve. This accords with the result of Berman [71] for stationary Gaussian sequences, that when z is large the EV statistics will converge to that of IID RVs drawn from the ED for any positive Δ.

To further elucidate this phenomenon, we need a different strategy that exploits the large-z expansion of the integral eigenvalue equation, i.e., Eq. (4). Expressing the largest eigenvalue as $\Lambda_*(z) \simeq 1-\phi(z)\Lambda_1(z)+[\phi(z)]^2\Lambda_2(z)$, and similarly for $P_*(x;z)$, we obtain [68]

$$\Lambda_*(z) \simeq 1 - \phi(z)\underbrace{\frac{\mathrm{erfc}(z/\sqrt{2})}{2\phi(z)}}_{\Lambda_1(z)} + [\phi(z)]^2\underbrace{\sum_{n=1}^{\infty}\frac{\mu^n/n!}{1-\mu^n}\mathrm{He}_{n-1}^2(z)}_{\Lambda_2(z)}, \tag{7}$$

where $\mathrm{He}_n(\cdot)$ is the nth probabilists' Hermite polynomial. Further expanding Eq. (7) for large z, we find

$$\Lambda_*(z) \simeq 1 - \frac{\phi(z)}{z} + \left[\frac{\phi(z)}{z}\right]^2 \frac{(1+\mu)^2}{\sqrt{1-\mu^2}} \exp\left(\frac{z^2\mu}{1+\mu}\right) \simeq 1 - \frac{\phi(z)}{z}\left(1 - \frac{2e^{-\Delta z^2/4}}{\sqrt{\pi\Delta z^2}}\right), \tag{8}$$

where the last expression is valid for small Δ [73]. Remarkably, the leading two terms are μ independent and correspond to the result for IID variables originating from the ED. However, for fixed z, when Δ becomes small, or equivalently μ approaches unity, the last term diverges, indicating the breakdown of the large-z perturbation theory and the existence of a crossover regime to a CS behavior for $\Delta z^2 \sim \mathcal{O}(1)$. This is evidenced in Fig. 3, where one sees that for small $T = \Delta N$, the distribution of z_{DS} is close to the CS prediction, whereas for large T it appears to converge to the IID limit. This transition has however nothing to do with a physical switch of the behavior of the system, and is rather a purely statistical effect due to the finite sampling rate. Thus, for any fixed $\Delta > 0$, as T becomes large the IID statistics and ED control the EV theory.

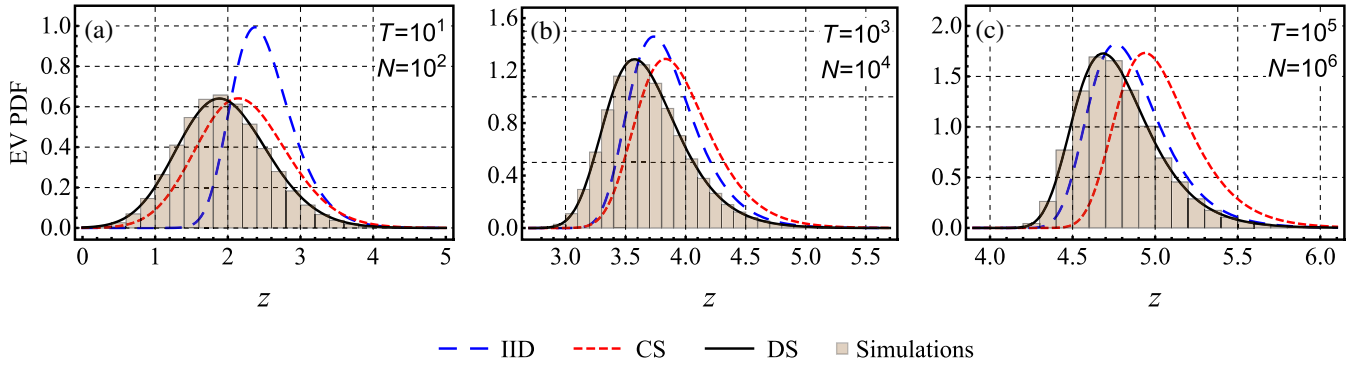

FIG. 3. The EV statistics of the DS OU model. The distribution of EVs for the DS OU process, with sampling rate $\Delta = 0.1$. For not too large T, we see a behavior close to that of the CS approach (a). However, as we increase T, approximating the DS statistics by those of CS becomes less accurate (b), and eventually approach the statistics predicted for $N = T/\Delta$ IID RVs drawn from the ED (c). The IID and DS curves (dashed blue and solid black) correspond to $\exp\{-N\ln[1/\Lambda(z)]\}$ with $\Lambda(z) = \Phi(z)$ and $\Lambda(z) = \Lambda_*(z)$, respectively. The CS curve (short-dashed red) corresponds to $\exp[-T\lambda_*(z)]$, where $\mathrm{D}_{\lambda_*(z)}(-z) = 0$. Each histogram is made of 10^6 maxima with initial conditions of $x = 0$.

A qualitative argument.—How are we to understand the crossover scale of $\Delta z^2 \sim \mathcal{O}(1)$? A simple explanation to this result is as follows. Let us expand the recursion relation of x_n for small Δ, $x_{n+1} - x_n \simeq -\Delta x_n + \sqrt{2\Delta}\eta_n$. We see that there is a competition between two terms. For small Δ the stochastic noise is dominant, and so a record-breaking large x_n is very liable to be followed by a yet larger value. However, for sufficiently large x_n, the deterministic term which is proportional to x_n dominates, so those maxima are separated by large gaps in time. These two terms are comparable precisely in the crossover regime we have identified. Physically, the effect we find here is related to the fact that extreme events of Langevin paths in a confining field become larger as time progresses. However, the bigger the true maximum is (in the CS sense), the faster the relaxation from this extreme gets, simply because the restoring force field gets enormously large if the path wanders to an EV. This idea suggests that our main result found for the OU process is of more general validity. We explore this by considering the path of a Brownian particle subjected to more general binding force fields. As explained below, these results extend beyond the Gumbel basin of attraction.

Other force fields in the Gumbel domain.—Let us consider a potential of the form $U(x) = (1/\alpha)(1 + x^2)^{\alpha/2}$, with $\alpha > 0$ (see further details in the Supplemental Material [68]). In Fig. 4, we plot the mean EV $\langle z \rangle$ versus T given various values of α. For the OU process with $\alpha = 2$, we see that the numerical values converge to the IID limit at large times; see Fig. 4(a). This works also for $\alpha = 2.5$, since here too the force grows with x, leading to a domination by the deterministic force term at long times. However, this argument is no longer valid for $\alpha \leq 1$, where the force does not increase with x; see Figs. 4(b) and 4(c). For example, when setting $\alpha = 0.5$, the stochastic term dominates at large x, and the exact values (which are nicely described by CS) diverge from the IID behavior; see Fig. 4(c). When $\alpha = 1$, the force is asymptotically constant, which is a special borderline case with all curves being parallel; see Fig. 4(b). This case was also shown to be critical for problems which do not involve DS; see Ref. [14] in the context of crowding of near-extreme events, and Ref. [74] where a freezing transition was discovered for the long-time decay rates of first-passage probabilities.

The Fréchet and Weibull EV limits.—Thus far, we have discussed processes with an asymptotic power-law potential. This means EDs of exponential type, so that their EV limits belong to the Gumbel class. However, our observations hold for the other two EV attractors as well. For the Fréchet class we observe a behavior similar to the Gumbel case with $\alpha < 1$. Namely, due to the force diminishing at infinity, the DS EV distribution agrees with the CS prediction. For the Weibull class we find that the DS EV distribution converges toward the IID prediction, diverging away from the CS limit. Key equations and supporting figures of these results appear in the Appendix, while derivations and additional extensions can be found in the Supplemental Material [68]. We thus conjecture that any process with a potential growing superlinearly, i.e., obeying $\lim_{x\to\infty} x/U(x) = 0$, will have its EV statistics controlled by the ED IID behavior in the long-time limit.

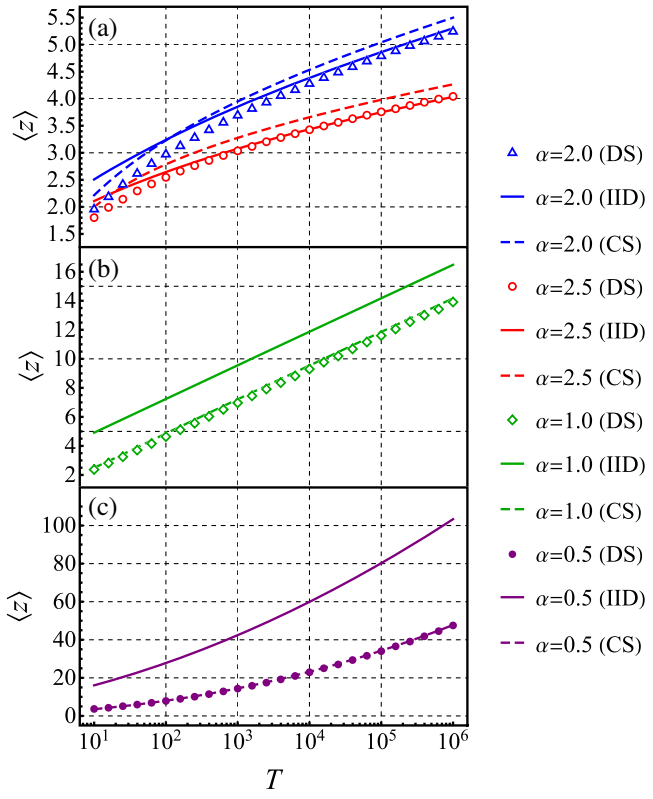

FIG. 4. The Gumbel class. The mean EV $\langle z \rangle$ of a DS process $x(t)$, evolving according to Eq. (1) ($D = 1$), but with a deterministic force of $-U'(x)$, where $U(x) = (1/\alpha)(1 + x^2)^{\alpha/2}$. We used (a) $\alpha = 2$ (blue triangles) and $\alpha = 2.5$ (red circles), (b) $\alpha = 1$ (green diamonds), and (c) $\alpha = 0.5$ (purple disks), corresponding to the OU model and to increasing, constant, and decreasing-force processes, respectively. Seen are numerical evaluations for these four cases, where the sampling interval is $\Delta = 0.1$. Also depicted are the ED IID (solid lines) and CS (dashed curves) predictions for each value of α. (a) For $\alpha > 1$, the DS values converge to the IID description. (c) The opposite happens for $\alpha < 1$, as this case has a force that vanishes for large distances. (b) The borderline case is $\alpha = 1$, where the DS, IID, and CS values do not seem to intersect. Each mean is made of 10^4 maxima whose initial conditions are $x = 0$, obtained using the Euler-Maruyama method with an underlying time increment of 0.01. A reflective boundary condition at $x = 0$ was used when $\alpha < 1$.

Summary and conclusions.—We have demonstrated how the difference between discrete and continuous sampling affects the extreme value (EV) distribution of correlated random variables (RV) generated from Langevin paths. For the Ornstein-Uhlenbeck process, we found that there is a crossover at large measurement times to the statistics of independent and identically distributed RVs drawn from the

equilibrium distribution, for any nonzero sampling interval. After providing an intuitive explanation for this phenomenon, we showed it holds for a class of potential fields that are strongly binding. We demonstrated that this is not true for the complementary cases, where the EV distribution diverges from that of independent and identically distributed RVs. Lastly, we showed that our findings apply also to the other two classical limits of EVs, Fréchet and Weibull, which were studied via two example cases.

The profound sensitivity of the EV theory of correlated continuous processes to the method of sampling suggests that similar effects will be present also in more general models. Further, any changes encountered in the statistics of EVs may be related to the sampling problem found here, and not to a real change in the physical properties of the system, as we explained. Exploring these issues for models such as fractional Brownian motion, continuous time random walks, processes with demographic or multiplicative noise, and statistics of first-passage times of discretely sampled processes remains an open challenge.

The support of the Israel Science Foundation via Grant No. 1614/21 is acknowledged.

Appendix: The Fréchet and Weibull EV limits.—We first consider a potential which grows logarithmically for large displacements [75–77], $U(x) = (\beta/2)\ln(1+x^2)$ with $\beta > 1$. Here, the Boltzmann-Gibbs ED decays as a power law; hence the IID limit belongs to the Fréchet class. Studying the mode z_0 of the EV distribution obtained from this Langevin process, we find that

$$z_0^{\mathrm{IID}} \sim N^{1/(\beta-1)}, \qquad z_0^{\mathrm{CS}} \sim T^{1/(\beta+1)}. \tag{A1}$$

Namely, the IID and CS limits in Eq. (A1) display different power-law decays (note that $T = N\Delta$). This is evidenced in Fig. 5, where for large Ts the CS limit dominates the EV distribution, whereas for small Ts the IID picture wins. The potential grows at infinity slower than linearly, hence the CS limit describes the EV distribution correctly at long times. See the Supplemental Material [68] for the complete derivation leading to Fig. 5.

Secondly, we consider a potential corresponding to a particle confined to a finite interval, $x(t) \in [0,1]$,

$$U(x) = (\gamma-1)\ln\left(\frac{1}{1-x}\right). \tag{A2}$$

Note that $\gamma = 1$, assuming reflective boundary conditions at $x = 0$ and $x = 1$, corresponds to a particle freely diffusing in a box. Since here the Boltzmann-Gibbs ED has a finite upper support point, the IID limit belongs to the Weibull class. As the particle's movement is bounded, its maximum value cannot exceed 1; hence it proves useful to study the quantity $1 - \langle z\rangle$, i.e., the deviation of the mean EV from its maximal possible value. Similarly to the Gumbel case with

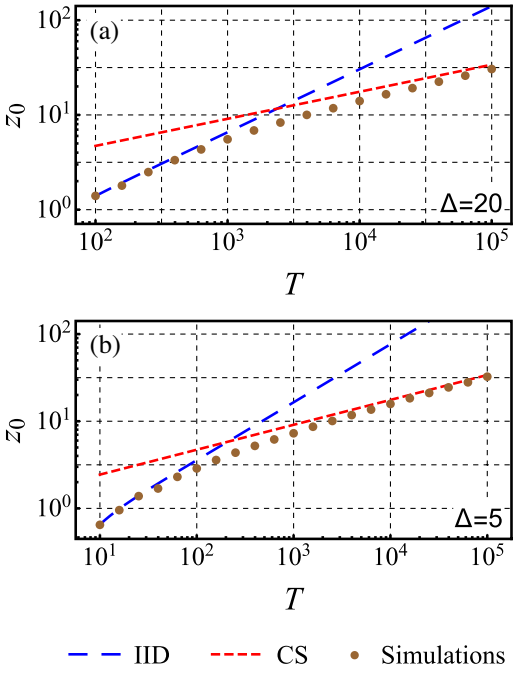

FIG. 5. The Fréchet class. The EV mode z_0 of a DS Langevin process $x(t)$, which evolves in time according to Eq. (1) ($D = 1$), but with a deterministic force of $-U'(x)$, where $U(x) = (\beta/2)\ln(1+x^2)$ and $\beta = 2.5$, for (a) $\Delta = 20$ and (b) $\Delta = 5$. Seen are stochastic simulations of the Langevin equation (brown disks), the IID limit (dashed blue line), and the CS limit (short-dashed red line). The CS limit dominates the DS EV distribution for large measurement times due to the force diminishing at $x \to \infty$, while for smaller Ts the IID limit prevails. Each mode was calculated by maximizing a tenth-order polynomial fitted to a probability density function constructed out of 10^5 EVs whose initial conditions are $x = 0$, obtained using the Euler-Maruyama method with an underlying time increment of 0.01 and a reflective boundary condition at $x = 0$.

$\alpha > 1$, the CS prediction is entirely off for large measurement times. In general, for the IID limit and any $\gamma > 0$, we find the following power-law decay rate:

$$1 - \langle z\rangle_{\mathrm{IID}} \sim N^{-1/\gamma}. \tag{A3}$$

However, for the CS limit and $\gamma > 2$, we obtain a different power law,

$$1 - \langle z\rangle_{\mathrm{CS}} \sim T^{-1/(\gamma-2)}, \tag{A4}$$

while for $0 < \gamma < 2$, the decay rate becomes exponential-like. Specifically for a particle freely diffusing in a box, where $\gamma = 1$, we obtain

$$1 - \langle z\rangle_{\mathrm{CS}} \sim \frac{8}{\pi^3 T}\exp\left(-\frac{\pi^2}{4}T\right). \tag{A5}$$

To illustrate these results, we first set $\gamma = 2.5$ in Fig. 6. Plotting the deviation of the mean EV from its maximal

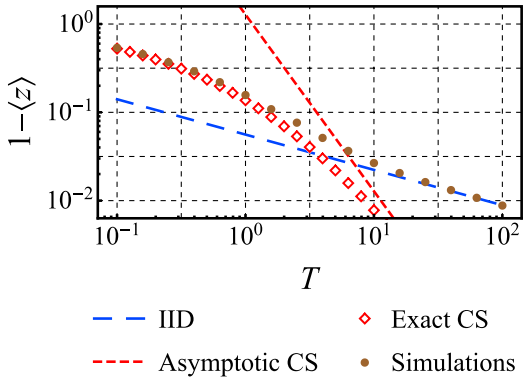

FIG. 6. The Weibull class. The deviation of the mean EV $\langle z\rangle$ from its maximal possible value for a DS Langevin process $x(t)$, which evolves in time according to Eq. (1) ($D = 1$), but with a deterministic force of $-U'(x)$, where $U(x)$ is given by Eq. (A2), $\gamma = 2.5$ and $\Delta = 10^{-3}$. Seen are stochastic simulations of the Langevin equation (brown disks), the IID limit (dashed blue line), the long-time asymptotics of the CS limit (short-dashed red curve), and the exact CS limit obtained numerically (hollow red squares). A clear transition from the CS limit to the IID prediction can be observed when the overall measurement time T is increased. Each mean is made of 10^4 maxima, whose initial conditions are $x = 0$, obtained using the Euler-Maruyama method with a varying underlying time increment with a maximal magnitude of 10^{-5}, and a reflective boundary condition at $x = 0$.

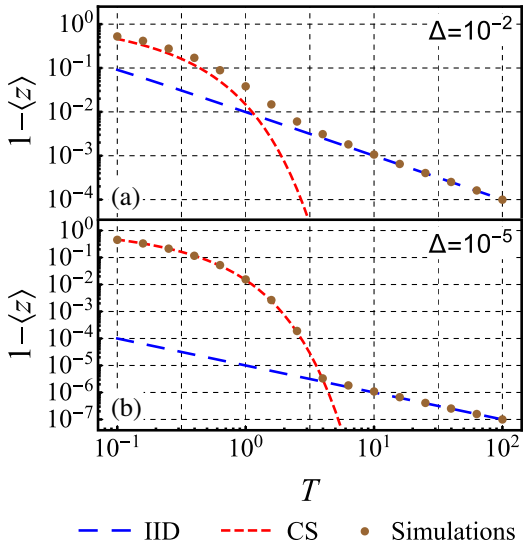

FIG. 7. A particle freely diffusing in a box. The deviation of the mean EV $\langle z\rangle$ from its maximal possible value for a free particle, namely $\gamma = 1$ in Eq. (A2), confined to [0, 1] and controlled by Eq. (1) (with $D = 1$ and a vanishing deterministic force). Seen are stochastic simulations of the Langevin equation (brown disks), the IID limit (dashed blue line), and the CS limit (short-dashed red curve). (a) For $\Delta = 10^{-2}$, a clear transition from the CS limit to the IID limit can be observed when the overall measurement time T is increased. (b) When decreasing Δ to 10^{-5}, the transition occurs at a larger T. Each mean is made of 10^4 maxima whose initial conditions are $x = 0$, obtained using the Euler-Maruyama method with an underlying time increment of 10^{-6} and reflective boundary conditions at $x = 0$ and $x = 1$.

possible value, $1 - \langle z\rangle$, versus the overall measurement time, T, we see that even if one takes a small sampling time of $\Delta = 10^{-3}$, the CS limit fails for large T, and the IID limit takes control of the EVs, with the ED as an underlying measure. For the other regime, we set $\gamma = 1$, giving the example of a particle freely diffusing in a box, as mentioned; see Fig. 7. It is clear that here too the CS limit fails for large T, while the IID limit works excellently. This again marks a qualitative difference between DS with any finite Δ to the CS limit of $\Delta = 0$, here for this example of particles freely diffusing in a box. The complete derivation leading to Figs. 6 and 7 can be found in the Supplemental Material [68].

*Corresponding author.
lior.zarfaty@mail.huji.ac.il

[1] E. J. Gumbel, *Statistics of Extremes* (Dover, New York, 1958).
[2] M. R. Leadbetter, G. Lindgren, and H. Rootzen, *Extremes and Related Properties of Random Sequences and Processes* (Springer-Verlag, New York, 1982).
[3] S. Kotz and S. Nadarajah, *Extreme Value Distributions: Theory and Applications* (Imperial College Press, London, 2000).
[4] S. Coles, *An Introduction to Statistical Modeling of Extreme Values* (Springer, London, 2001).
[5] L. de Haan and A. Ferreira, *Extreme Value Theory: An Introduction* (Springer, New York, 2006).
[6] J. P. Bouchaud and M. Mézard, J. Phys. A **30**, 7997 (1997).
[7] D. S. Dean and S. N. Majumdar, Phys. Rev. E **64**, 046121 (2001).
[8] T. Antal, M. Droz, G. Györgyi, and Z. Rácz, Phys. Rev. Lett. **87**, 240601 (2001).
[9] S. N. Majumdar and P. L. Krapivsky, Phys. Rev. E **65**, 036127 (2002).
[10] A. Comtet and S. N. Majumdar, J. Stat. Mech. (2005) P06013.
[11] E. Bertin, Phys. Rev. Lett. **95**, 170601 (2005).
[12] E. Bertin and M. Clusel, J. Phys. A **39**, 7607 (2006).
[13] D. S. Dean and S. N. Majumdar, Phys. Rev. Lett. **97**, 160201 (2006).
[14] S. Sabhapandit and S. N. Majumdar, Phys. Rev. Lett. **98**, 140201 (2007).
[15] G. Biroli, J. P. Bouchaud, and M. Potters, J. Stat. Mech. (2007) P07019.
[16] D. S. Dean and S. N. Majumdar, Phys. Rev. E **77**, 041108 (2008).
[17] M. R. Evans and S. N. Majumdar, J. Stat. Mech. (2008) P05004.
[18] Y. V Fyodorov and J. P. Bouchaud, J. Phys. A **41**, 372001 (2008).
[19] G. Györgyi, N. R. Moloney, K. Ozogány, and Z. Rácz, Phys. Rev. Lett. **100**, 210601 (2008).
[20] S. N. Majumdar and R. M. Ziff, Phys. Rev. Lett. **101**, 050601 (2008).
[21] S. N. Majumdar, A. Comtet, and J. R. Furling, J. Stat. Phys. **138**, 955 (2010).

[22] G. Györgyi, N. R. Moloney, K. Ozogány, Z. Rácz, and M. Droz, Phys. Rev. E **81**, 041135 (2010).
[23] E. Bertin, J. Phys. A **43**, 345002 (2010).
[24] E. Bertin and G. Györgyi, J. Stat. Mech. (2010) P08022.
[25] I. I. Eliazar and I. M. Sokolov, Physica (Amsterdam) **389A**, 4462 (2010).
[26] G. Wergen, J. Phys. A **46**, 223001 (2013).
[27] J. Y. Fortin and M. Clusel, J. Phys. A **48**, 183001 (2015).
[28] A. Bar, S. N. Majumdar, G. Schehr, and D. Mukamel, Phys. Rev. E **93**, 052130 (2016).
[29] O. Bénichou, P. L. Krapivsky, C. Mejía-Monasterio, and G. Oshanin, Phys. Rev. Lett. **117**, 080601 (2016).
[30] D. Hartich and A. Godec, J. Phys. A **52**, 244001 (2019).
[31] A. Vezzani, E. Barkai, and R. Burioni, Phys. Rev. E **100**, 012108 (2019).
[32] W. Buijsman, V. Gritsev, and V. Cheianov, Phys. Rev. B **100**, 205110 (2019).
[33] W. Wang, A. Vezzani, R. Burioni, and E. Barkai, Phys. Rev. Research **1**, 033172 (2019).
[34] S. N. Majumdar, A. Pal, and G. Schehr, Phys. Rep. **840**, 1 (2020).
[35] M. Höll, W. Wang, and E. Barkai, Phys. Rev. E **102**, 042141 (2020).
[36] C. Godrèche, J. Stat. Phys. **182**, 13 (2021).
[37] D. S. Grebenkov, V. Sposini, R. Metzler, G. Oshanin, and F. Seno, New J. Phys. **23**, 023014 (2021).
[38] L. Zarfaty, E. Barkai, and D. A. Kessler, J. Phys. A **54**, 315205 (2021).
[39] B. De Bruyne, S. N. Majumdar, and G. Schehr, J. Stat. Mech. (2021) 083215.
[40] F. Mori, S. N. Majumdar, and G. Schehr, Europhys. Lett. **135**, 30003 (2021).
[41] P. C. Y. Chen and Y. C. Fung, Microvasc. Res. **6**, 32 (1973).
[42] P. W. Burton, Geophys. J. Int. **59**, 249 (1979).
[43] F. Rossi, M. Fiorentino, and P. Versace, Water Resour. Res. **20**, 847 (1984).
[44] D. Sornette, L. Knopoff, Y. Y. Kagan, and C. Vanneste, J. Geophys. Res. **101**, 13883 (1996).
[45] P. Embrechts, C. Klüppelberg, and T. Mikosch, *Modelling Extremal Events for Insurance and Finance* (Springer, Berlin, 1997).
[46] P. Embrechts, S. I. Resnick, and G. Samorodnitsky, N. Am. Actuar. J. **3**, 30 (1999).
[47] R. W. Katz, M. B. Parlange, and P. Naveau, Adv. Water Resour. **25**, 1287 (2002).
[48] H. A. Orr, Genetics **163**, 1519 (2003).
[49] P. Naveau, M. Nogaj, C. Ammann, P. Yiou, D. Cooley, and V. Jomelli, C. R. Geoscience **337**, 1013 (2005).
[50] G. Gradoni and L. R. Arnaut, IEEE Transactions on Electromagnetic Compatibility **52**, 506 (2010).
[51] E. Castillo, *Extreme Value Theory in Engineering* (Elsevier, New York, 2012).
[52] S. M. Papalexiou and D. Koutsoyiannis, Water Resour. Res. **49**, 187 (2013).
[53] E. Ben-Naim, E. G. Daub, and P. A. Johnson, Geophys. Res. Lett. **40**, 3021 (2013).
[54] I. A. Chaves and R. E. Melchers, Struct. Saf. **50**, 9 (2014).
[55] L. Cheng, A. AghaKouchak, E. Gilleland, and R. W. Katz, Clim. Change **127**, 353 (2014).
[56] D. K. Dey and J. Yan, *Extreme Value Modeling and Risk Analysis: Methods and Applications* (CRC Press, Boca Raton, 2016).
[57] J. Osterrieder and J. Lorenz, Ann. Financ. Econ. **12**, 1750003 (2017).
[58] Z. Schuss, K. Basnayake, and D. Holcman, Phys. Life Rev. **28**, 52 (2019).
[59] L. H. C. Tippett and R. A. Fisher, Proc. Cambridge Philos. Soc. **24**, 180 (1928).
[60] E. J. Gumbel, Ann. Inst. Henri Poincaré **5**, 115 (1935).
[61] B. V. Gnedenko, Ann. Math. **44**, 423 (1943).
[62] P. Hall, J. Appl. Probab. **16**, 433 (1979).
[63] R. Giuliano and C. Macci, Commun. Stat. **43**, 1077 (2014).
[64] B. V. Gnedenko and A. N. Kolmogorov, *Limit Distributions for Sums of Independent Random Variables* (Addison-Wesley, Cambridge, 1968).
[65] M. J. Kearney and R. J. Martin, J. Phys. A **54**, 055002 (2021).
[66] J. Pickands, Probab. Theory Relat. Fields **7**, 190 (1967).
[67] D. T. Gillespie, Phys. Rev. E **54**, 2084 (1996).
[68] See Supplemental Material at http://link.aps.org/supplemental/10.1103/PhysRevLett.129.094101 for (I) Further details regarding Eq. (4); (II) Derivation of Eqs. (7) and (8); and (III) Langevin processes with non-linear forces, which includes Ref. [69].
[69] B. V. Bondarev, Appl. Math. **8**, 1529 (2017).
[70] Note that in Ref. [34], a typographical error resulted in an extra factor of two (S. N. Majumdar, private communication).
[71] The convergence of the extreme value distribution of stationary Gaussian sequences to its independent and identically distributed limit was previously obtained in S. M. Berman, Ann. Math. Stat. **35**, 502 (1964). However, the connection to continuous stationary Gaussian processes, as well as the singular nature of the $\Delta \to 0$ limit, were overlooked.
[72] Wolfram Research Inc., Mathematica, Version 12.1.1, Champaign, IL (2020).
[73] Note that taking $\Delta \to 0$ as discussed before and shown in Eq. (5) yields the CS limit for any finite z. Likewise, the $z \to \infty$ limit in Eq. (8) holds for any finite Δ, where the relevant threshold is determined by the crossover scale of $z^2\Delta \sim O(1)$. However, these limits do not commute, and so the large-z limit of Eq. (5) is different from the small-Δ limit of Eq. (8).
[74] S. Sabhapandit and S. N. Majumdar, Phys. Rev. Lett. **125**, 200601 (2020).
[75] H. C. Fogedby and R. Metzler, Phys. Rev. Lett. **98**, 070601 (2007).
[76] A. Dechant, E. Lutz, E. Barkai, and D. A. Kessler, J. Stat. Phys. **145**, 1524 (2011).
[77] O. Hirschberg, D. Mukamel, and G. M. Schütz, Phys. Rev. E **84**, 041111 (2011).